Extended Abstract

Doctoral Thesis in Environmental Engineering, Mining and Energy

Economic and environmental analysis of applying ammonia as carbon free fuel in internal combustion engine driven agricultural vehicle performed in whole life cycle approach

Mateusz Proniewicz

Silesian University of Technology
Gliwice, Poland, 2025

Author:
mgr inż. Mateusz Proniewicz
Department of Thermal Technology, Faculty of Energy and Environmental Engineering, Silesian University of Technology
e-mail: mateusz.proniewicz@polsl.pl

Supervisor:
prof. dr hab. inż. Andrzej Szlęk
Department of Thermal Technology, Faculty of Energy and Environmental Engineering, Silesian University of Technology
e-mail: andrzej.szlek@polsl.pl

Co-supervisor:
dr inż. Karolina Petela
Department of Thermal Technology, Faculty of Energy and Environmental Engineering, Silesian University of Technology
e-mail: karolina.petela@polsl.pl

Chapter 1 – Introduction

Energy use is one of the pillars of civilization's development. Global direct primary energy consumption has continuously grown, from 27 972 TWh in 1950 to 167 584 TWh in 2024. This energy is primarily supplied by fossil fuels: gas, oil, and coal accounted for 72 % of global direct primary energy in 1950, increasing to 85 % in 2024 [1]. However, intensive exploitation of fossil fuels is linked to greenhouse gas (GHG) emissions, which in turn affect the climate. In this context, hydrogen has gained interest as a versatile energy carrier that can replace existing fuels. It is characterized by a high lower heating value (LHV) on a mass basis (2.4 times higher than methane [2]), no carbon emissions upon combustion, and renewability when produced by water electrolysis using renewable electricity [3]. However, for mobile applications hydrogen poses a challenge for efficient storage: it can be stored either as a liquid at low temperatures (saturation temperature around −253 °C at 1 bar [4]) or as a gas under high pressure (700 bar) [5]. From this perspective, ammonia emerges as a promising alternative. Similar to hydrogen, its molecule contains no carbon atoms and therefore its combustion does not emit carbon dioxide. It is mainly produced in the Haber–Bosch process [14] by reacting hydrogen with nitrogen; given that nitrogen is obtained from air, ammonia can be classified as renewable if renewable hydrogen is used. Ammonia's saturation temperature is around −34 °C at 1 bar [6], and its storage is therefore much more feasible than that of hydrogen; when pressurized to 20 bar, it remains liquid up to 50 °C [7]. From an internal combustion engine (ICE) perspective, although ammonia's lower heating value per kilogram of fuel is about 44 % of that of diesel [8], its lower stoichiometric air–fuel ratio results in a similar energy content per kilogram of stoichiometric fuel–air mixture (2.64 vs 2.77 MJ/kg-mixture) [8]. Thus, for the same amount of air inducted into the engine, a comparable amount of energy can be delivered using ammonia as in the case of diesel fuel.

However, this raises questions about the environmental and economic implications of such a fuel switch when assessed from a life cycle perspective. If the engine were fueled by pure ammonia, no carbon emissions would be produced during its operation. However, since ammonia has a lower energy content per kilogram of fuel than diesel, a greater amount of ammonia must be consumed to deliver the same output. If ammonia production had a high environmental impact due to intensive energy or resource use, resulting in considerable GHG emissions, the benefits of reducing GHG emissions during the vehicle's operation phase could be offset or even exceeded by the emissions associated with ammonia production. Next aspect is that due to the challenges of pure ammonia combustion, dual-fuel operation has been considered to achieve stable engine operation, in line with literature suggestions [9], with biodiesel serving as the pilot fuel. Detailed analysis of engine emissions considering dual-fuel operation under varying load is essential for a complete understanding of the fuel switch. Since ammonia combustion can lead, among others, to nitrous oxide (N_2O) emissions [10], [11], which is a potent GHG with a Global Warming Potential (GWP) of 273 [12], this factor must be accounted for. Finally, another aspect of the fuel switch is the

economic comparison between the two options, specifically the expenditure required to purchase and operate a diesel- or ammonia-fueled vehicle, noting that the cost of ammonia depends on the source of hydrogen.

To address these research questions, the specific objectives of this work can be formulated as follows:

1. Defining the differences between the impact on the environment of ammonia- and diesel-fueled mini tractor based on life cycle assessment (LCA).
2. Assessing the economic performance of ammonia- and diesel-fueled mini tractor based on life cycle costing (LCC).

Life Cycle Assessment (LCA) and Life Cycle Costing (LCC) quantify, respectively, the environmental impacts and total costs of a given product or asset throughout its lifespan, i.e., from production/acquisition through operation with maintenance to end of life (EoL) [13], [14]. A hectare-year of tractor operation has been selected as the functional unit. The LCA was performed using the LCA for Experts software (formerly GaBi). For the ammonia-fueled case, the fuel production stage covers the complete ammonia production pathway for several scenarios, from fossil- to renewable-based routes, while the tractor operation stage reflects emissions obtained from experimental measurements of the ammonia-fueled engine. The system boundaries are shown in Figure 1. For the diesel-fueled LCA, fuel production pertains to diesel, and emissions are based on experiments from diesel-fueled engine. The same assumptions are applied to estimate the environmental impact of tractor production and disposal (EoL) in both fuel cases.

The life cycle inventory is based on primary experimental data for the operation phase and secondary data for the remaining phases. Secondary data are drawn from Sphera's Managed LCA Content database [15] and the literature; the database is based on industry data, with reliability ensured by third-party review. Life cycle impact assessment uses selected environmental categories according to the ReCiPe method (midpoint: climate change, fossil depletion, freshwater consumption; endpoint: human health, ecosystem quality), followed by interpretation. While LCA is standardized at the framework level, its application in this study required several case-specific developments, including defining tractor- and orchard-specific system boundaries and operating scenario, constructing consistent life cycle inventories by collecting and processing primary experimental data for the ammonia- and diesel-fueled engine, and aggregating secondary data for fuel production pathways and other life cycle phases.

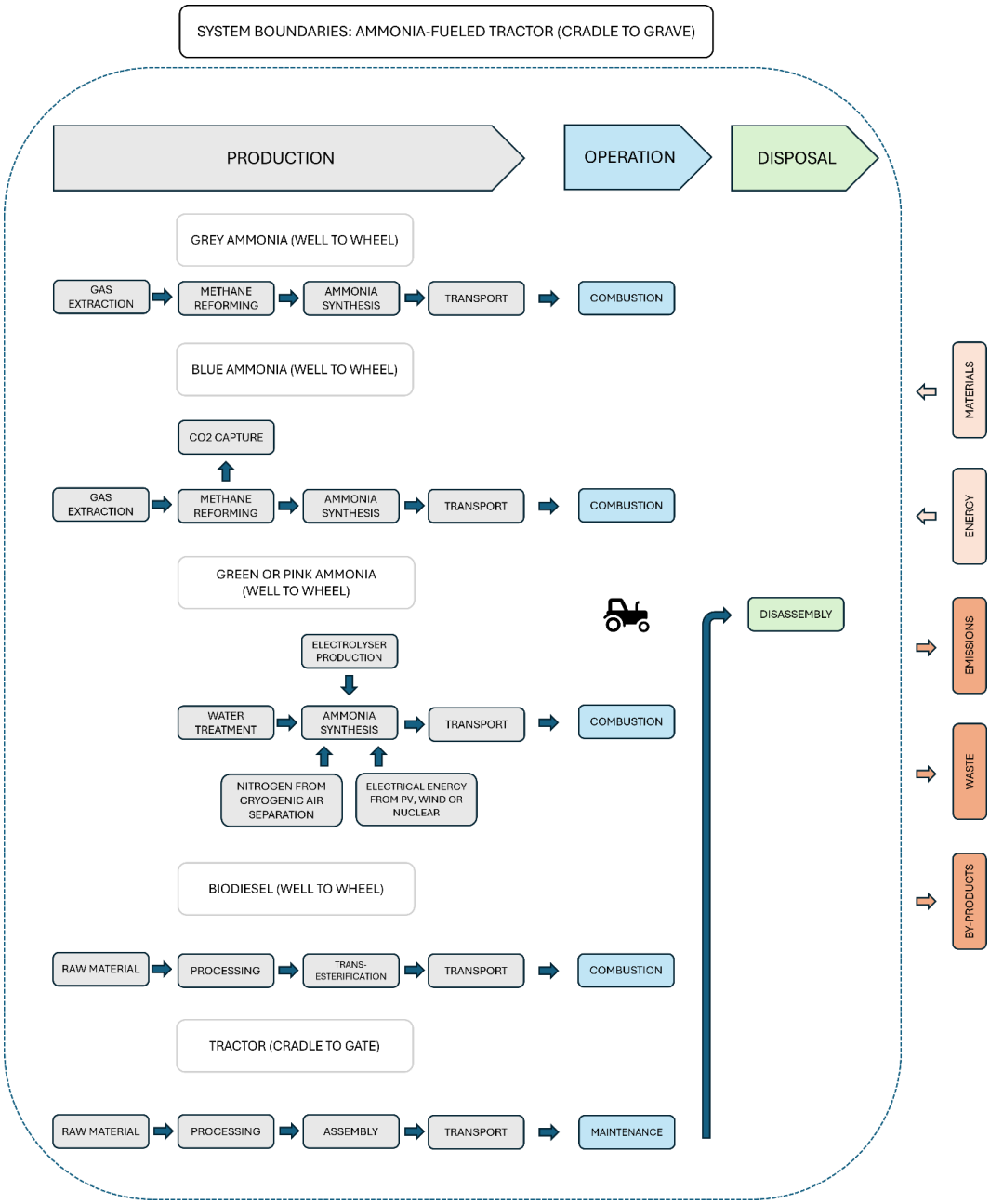

Figure 1. System boundaries for the LCA of an ammonia-fueled mini-tractor.

The structure of the life cycle costing (LCC) follows the LCA approach; an overview of the LCC system boundaries is shown in Figure 2. For the ammonia-fueled mini tractor, tractor acquisition corresponds to the price of a standard mini tractor with a compression ignition engine, additionally equipped with a port injection system for ammonia utilization; the pilot fuel uses a direct injection setup with biodiesel substituting diesel. For the reference diesel-fueled case, tractor acquisition is represented by the market price of a conventional diesel tractor. The operation phase includes fuel expenditure – considering ammonia from both fossil and renewable pathways – as well as vehicle maintenance. Tractor disposal covers the cost of disposing of the vehicle body.

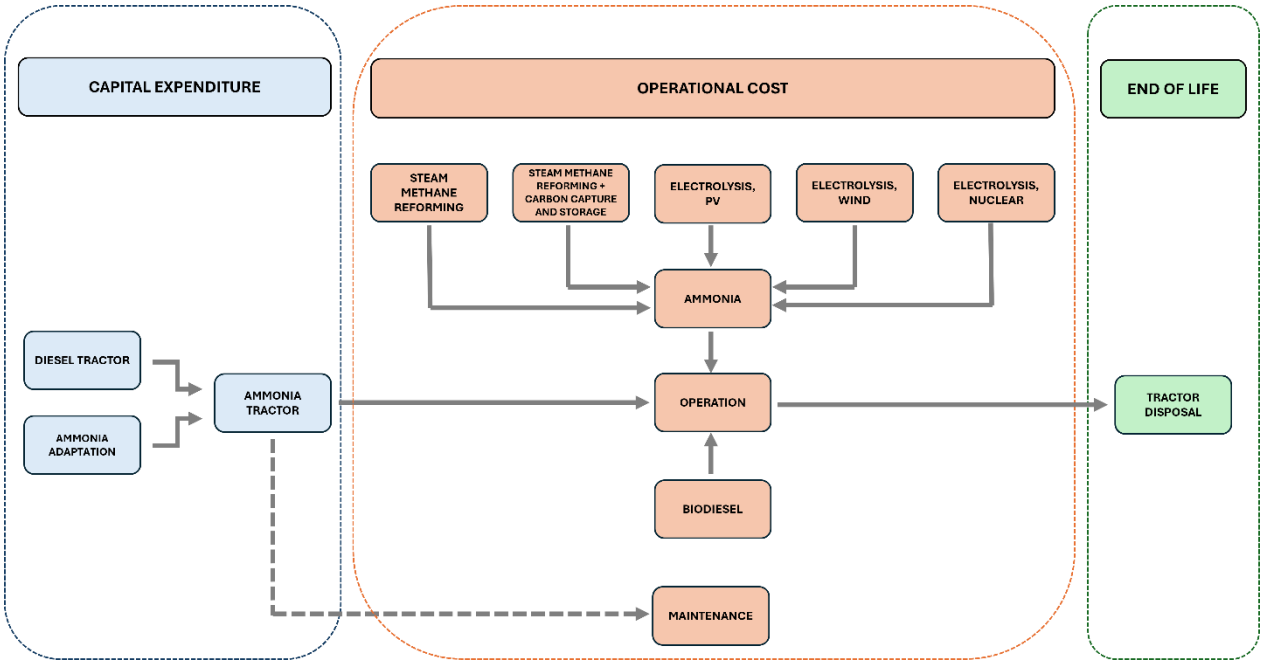

Figure 2. System boundaries for the LCC of an ammonia-fueled mini-tractor.

Chapter 2 elaborates on the environmental impacts of several ammonia production pathways through a dedicated LCA; Chapter 3 discusses experimental engine data. Chapter 4 presents a full LCA of an ammonia-fueled mini tractor versus a diesel reference, using results from Chapters 2 and 3, and addresses the first objective of the thesis. Chapter 5 conducts the LCC comparison between ammonia- and diesel-fueled mini tractor, addressing the second objective, and Chapter 6 summarizes and concludes the main findings.

Chapter 2 – Ammonia production pathways

The primary industrial method for ammonia production is the Haber–Bosch process, valued for its technological maturity and scalability [16], [17] and used here as the reference route. It is based on the exothermic reaction of nitrogen with hydrogen. Since nitrogen is obtained from atmospheric air, the hydrogen source determines the ammonia type, according to the following naming:

i. Grey ammonia – hydrogen from steam methane reforming (SMR)
ii. Blue ammonia – hydrogen from SMR with carbon capture and storage
iii. Green ammonia – hydrogen from water electrolysis powered by solar PV or wind
iv. Pink ammonia – hydrogen from water electrolysis powered by nuclear energy

To evaluate the environmental performance of ammonia as a fuel, a cradle to gate analysis (from raw material extraction to ammonia production) was conducted with a functional unit of 1 MJ

(LHV). The environmental impact of grey and blue ammonia has been estimated directly based on aggregated processes available in the database accessible in the software used to perform the analysis. Green ammonia has been modeled independently, using an alkaline electrolyzer, as the most representative technology (60 % of installed capacity in 2023 [10]), with a literature-based electrolysis model and upstream processes from the software database. Three electricity cases are assessed – PV and wind (green ammonia) and nuclear (pink ammonia) – with identical process parameters. As ammonia is compared with diesel as an ICE fuel, diesel production is included as a reference.

Figure 3 compares the five ammonia routes with diesel across three midpoint indicators on a normalized scale. For climate change, the ranking among ammonia options is: grey, blue, green PV, green wind, pink. Relative to diesel production alone, green wind and pink show lower values (pink at about half of diesel). Because the functional unit is 1 MJ (LHV), diesel's production footprint is relatively small, as a smaller amount of diesel is required to provide 1 MJ compared to ammonia. However, when diesel is used in an ICE, combustion dominates its climate impact, so a scenario including stoichiometric combustion CO_2 is added. Grey ammonia is the only route exceeding this total, confirming that SMR-based ammonia is not climate benign; blue is lower but still substantial, as CCS targets only part of involved CO_2 emissions. Green and pink routes are preferred overall, with PV the least favorable of the three electricity cases. For fossil depletion, both green routes are lowest; diesel, grey, and blue are at intermediate levels, while pink is highest. Freshwater consumption is dominated by the nuclear (pink) case, whereas diesel has the lowest value.

Figure 4 presents endpoint results for human health and ecosystem quality (terrestrial, freshwater, and marine) on a normalized scale. Human health largely follows the climate change pattern: pink is lowest, followed by green wind and green PV; diesel production alone is also low but increases when combustion is included; grey is highest and blue lies in between. Ecosystem quality is mainly driven by the terrestrial component. Green PV shows the largest terrestrial impact, reflecting the material-intensive nature of PV manufacturing and end of life treatment, while wind, pink, blue, and grey cluster at similar, lower levels, with diesel lowest; the differences are modest except for PV. For freshwater ecosystems, the spread is small: diesel including combustion is highest, and green wind is lowest. For marine ecosystems, grey ammonia is highest; diesel including combustion follows at roughly five times lower, and green wind again shows the lowest impact.

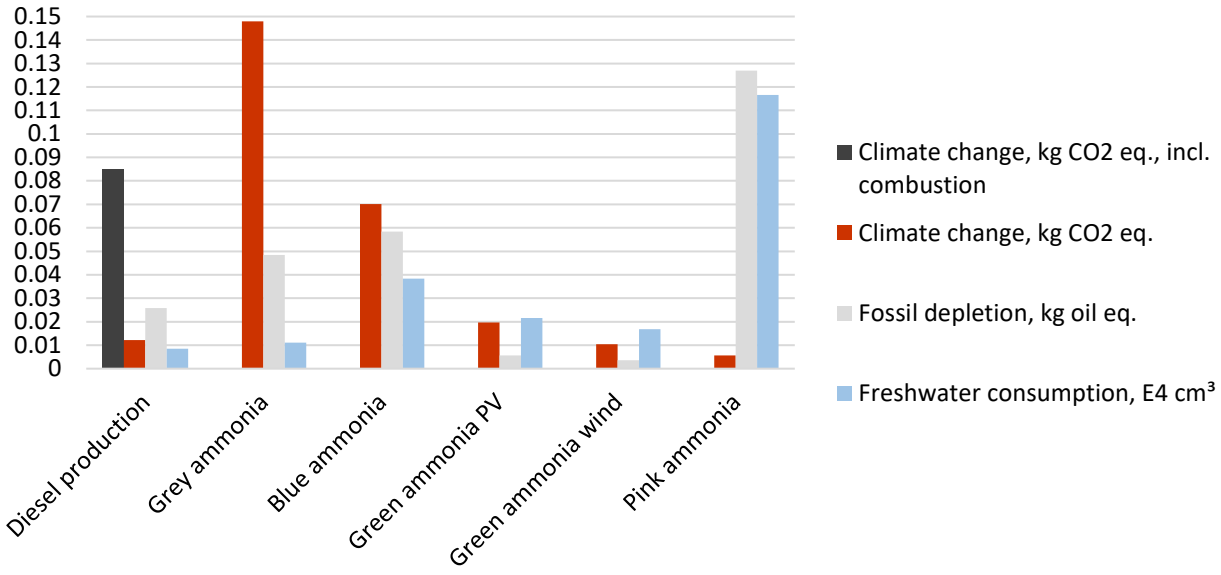

Figure 3. Midpoint category results for ammonia production pathways.

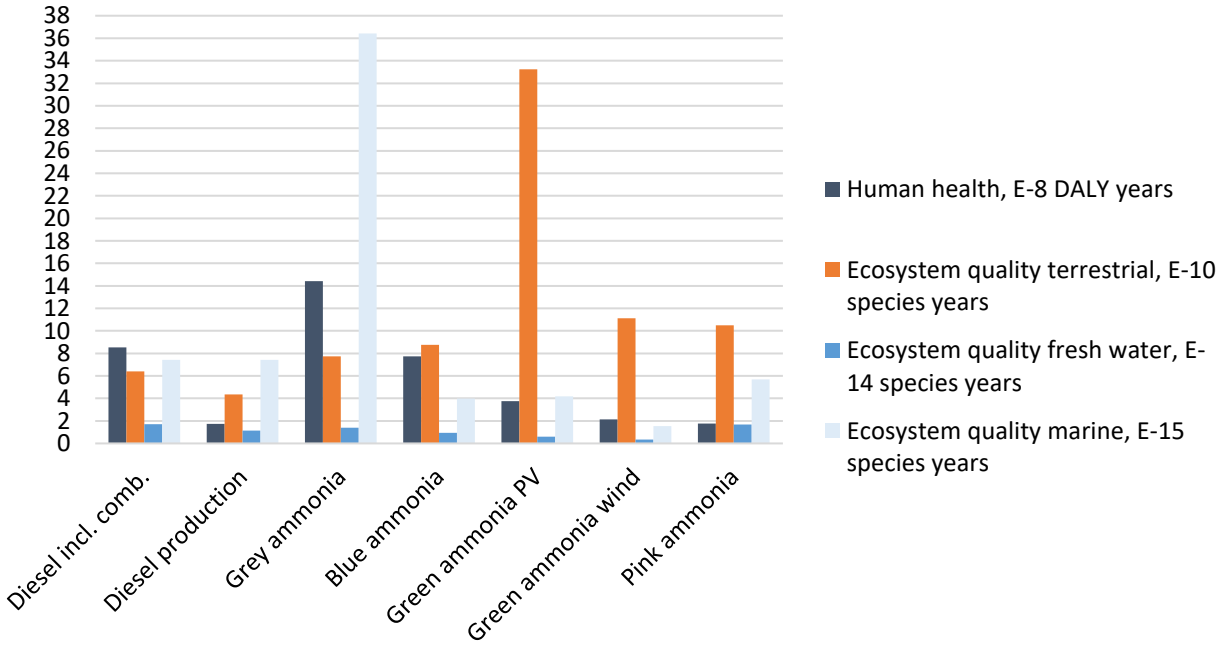

Figure 4. Endpoint category results for ammonia production pathways.

Chapter 3 – Ammonia- and diesel-fueled engine performance

Experiments were carried out on a Lifan C186F single cylinder mini tractor engine. Ammonia was supplied to the engine by gaseous port injection into the intake manifold, where it was premixed

with air, while biodiesel was injected directly as the pilot fuel. A schematic of the test rig is shown in Figure 5. NH_3 mass flow rate was measured using a Coriolis meter, while air volumetric flow rate was measured using a turbine flowmeter. Air, fuel, and exhaust temperatures were recorded with thermocouples. Shaft torque and speed were controlled using an electric machine operated as a brake. All signals were acquired and controlled in LabVIEW. Exhaust composition was measured on a wet basis using FTIR (Gasmet DX4000), with additional O_2 measurement (CAPELEC CAP 3201) and PM10 verification (SMG200 M). Recorded variables included fuel consumption and concentrations of CO_2, CO, CH_4, NO_x, NH_3, SO_2, PM10, and other exhaust species. Major engine characteristics and fuel elemental compositions with LHV are given in Table 1.

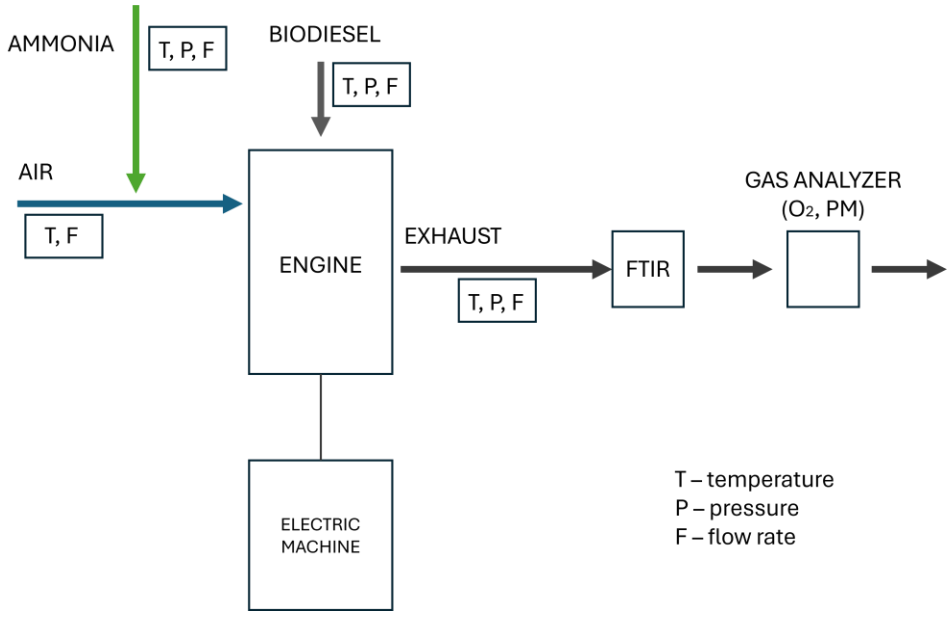

Figure 5. Schematic of the test rig used in the experiments.

Table 1. Engine and fuel characteristics.

Engine	Model: LIFAN C186F, 4-stroke, 1-cylinder, forced air cooling Displacement: 418 cm^3 Compression ratio: 16.5:1 Max theoretical power: 6.4 kW
Diesel	C = 0.8078, H = 0.1556, O = 0.0363, N = 0.0003 LHV = 42.4 MJ/kg
Biodiesel	C = 0.7533, H = 0.1397, O = 0.1070, N = 0.0000 LHV = 37.4 MJ/kg
Ammonia	C = 0.0000, H = 0.1760, O = 0.0000, N = 0.8240 LHV = 18.6 MJ/kg

Tests covered shaft speeds of 2700, 2400, 2100, 1800, 1500, and 1200 rpm. At 2700 rpm, torques of 12, 8, and 4 Nm were applied; at the other speeds, torques of 17, 12, 8, and 4 Nm were used. For ammonia operation, the biodiesel mass flow rate was fixed at the minimum value that ensured stable combustion (corresponding to 4 Nm), and increasing the NH_3 flow increased torque. The operating point 2700 rpm / 12 Nm represented the upper limit for ammonia operation. Fuel consumptions and greenhouse gas emissions in CO_2 equivalents – combining CO_2 (GWP = 1), CH_4 (GWP = 27), and N_2O (GWP = 273) – for diesel and ammonia operation are summarized in Table 2. Due to relatively high N_2O emissions under some conditions, there are operating points where total GHG emissions from the ammonia-fueled engine exceed those of the diesel case (e.g., 2700 rpm at all loads, 2400 rpm at 12 and 8 Nm). This shows that whether the fuel switch achieves its primary decarbonization purpose depends strongly on engine operating conditions.

Table 2. Comparison of fuel consumption and GHG emissions for ammonia- and diesel-fueled operation (D = diesel; A = ammonia).

RPM, 1/min	Load, Nm	Diesel (D), g/s	Biodiesel, g/s (A)	Ammonia, g/s (A)	GHG, CO2 eq./s (D)	GHG, CO2 eq./s (A)
2700	12.00	0.323	0.202	0.412	0.951	1.012
2700	8.00	0.249	0.203	0.232	0.733	1.126
2700	4.00	0.180	0.195	0.000	0.523	0.529
2400	17.00	0.400	0.184	0.492	1.152	0.871
2400	12.00	0.277	0.182	0.346	0.815	0.856
2400	8.00	0.220	0.181	0.175	0.648	0.996
2400	4.00	0.164	0.170	0.000	0.475	0.464
2100	17.00	0.334	0.154	0.480	0.979	0.728
2100	12.00	0.243	0.156	0.317	0.719	0.715
2100	8.00	0.182	0.155	0.169	0.537	0.893
2100	4.00	0.134	0.147	0.000	0.391	0.401
1800	17.00	0.291	0.129	0.428	0.842	0.653
1800	12.00	0.205	0.128	0.281	0.604	0.680
1800	8.00	0.156	0.132	0.142	0.461	0.823
1800	4.00	0.111	0.126	0.000	0.325	0.345
1500	17.00	0.252	0.111	0.356	0.723	0.548
1500	12.00	0.178	0.110	0.237	0.525	0.561
1500	8.00	0.134	0.111	0.124	0.397	0.672
1500	4.00	0.094	0.107	0.000	0.276	0.293
1200	17.00	0.214	0.093	0.284	0.604	0.442
1200	12.00	0.153	0.093	0.193	0.448	0.441
1200	8.00	0.110	0.091	0.105	0.324	0.520
1200	4.00	0.079	0.088	0.000	0.232	0.241

Chapter 4 – LCA of an ammonia-fueled mini tractor

Environmental impact of a mini tractor production is modeled using a process from Sphera's Managed LCA Content dataset; fuel production pathways follow the approach elaborated in Chapter 2. As the engine operates in dual-fuel mode, biodiesel production is included to complete the LCA, in line with Figure 1. Biodiesel is modeled via transesterification of oils/fats with methanol using a literature-based inventory [18], assuming a supercritical methanol route with a propane co-solvent. Transport of biodiesel and ammonia, prior to their use in ICE, is modeled as 150 km by road in a Euro V freight truck. The EoL phase is represented by the car shredder process from the software database [15].

Because the engine is sized for a mini tractor used in orchard operations and emissions depend on operating conditions, the engine working cycle must be characterized in detail. First, typical orchard activities and their annual frequencies for a representative apple orchard were obtained from the literature [19]. Next, a scaled CAD model of the orchard was developed to simulate tractor movement for tasks such as sweeping, hoeing, mowing, spraying, harvesting, and pruning. A theoretical gearbox operation model was then defined: activities were divided into sub-activities (e.g., driving to the orchard on a gravel road, turning, driving through alleys), and gear–speed combinations were assigned to each. Considering mini tractor characteristics, rolling resistance, air drag, and activity type, engine speed and torque were derived. Using these operating points and the experimental engine map, fuel consumption and emissions were obtained by interpolation from the measured data, which constitutes the operation phase of the LCA.

Climate change results are shown in Figure 6 (a). Reference fuel production pertains to diesel for the diesel-fueled vehicle and biodiesel for the ammonia-fueled vehicle. For the diesel-fueled mini tractor, vehicle operation dominates the impact (ca. 70 %), followed by tractor and diesel production; end of life is negligible. The operational burden is driven mainly by CO_2, with contributions from CH_4 and N_2O. Next factor is ammonia production. In the blue case (SMR with CCS), emissions from ammonia production are about half of those in the grey case; electrolysis-based routes reduce them further, with pink (nuclear) lowest. For all ammonia-fueled scenarios, operation is also the main contributor. Ammonia operation emits less CO_2 (non-zero due to the biodiesel pilot) but more N_2O than diesel, which affects the GHG balance. Over the duty cycle, the ammonia tractor emits about 72 kg CO_2 eq., compared with about 88 kg CO_2 eq. for diesel, which is an 18 % reduction. The third contributor is pilot fuel (biodiesel) production. Biogenic CO_2 uptake in rapeseed cultivation is credited, giving biodiesel a negative climate impact and further improving the overall balance. Tractor production is identical in all scenarios, and the retrofit (NH3 tank and line) increases vehicle mass by less than 5 %, so its effect on production impacts is negligible. Aggregated results in Figure 6 (b) show the largest GHG reductions for electrolysis-based ammonia from wind and nuclear, at about 42 % and 44 %, respectively, relative to diesel.

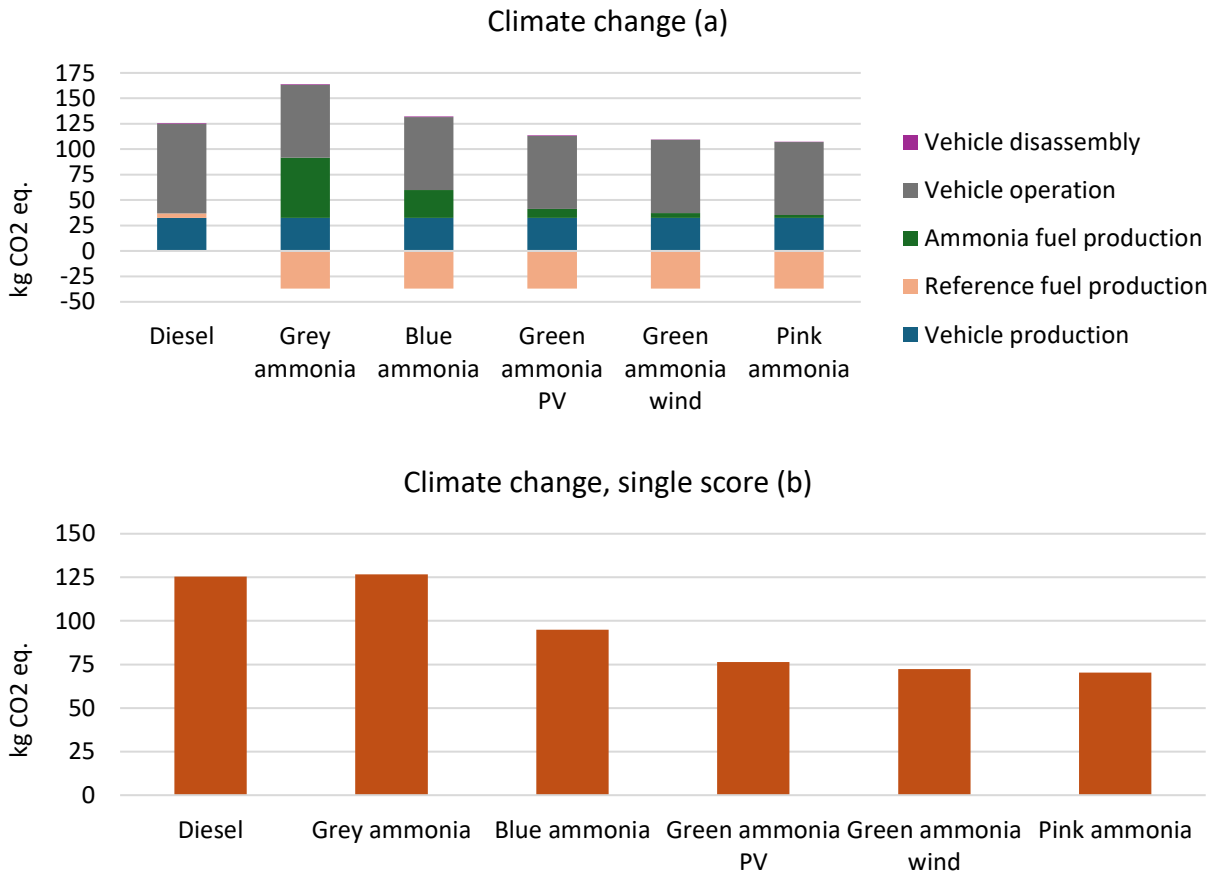

Figure 6. Climate change results.

Fossil depletion results (Figure 7 (a)) are driven by fuel pathways and vehicle manufacturing. Grey ammonia (SMR) is comparable to diesel, while blue (SMR + CCS) is slightly higher due to the CCS burden. Renewable ammonia has the lowest fossil depletion, with reductions of about 43 % (PV) and 45 % (wind) versus diesel. The nuclear route is 78 % higher than diesel, reflecting high uranium resource use. Biodiesel contributes to fossil depletion through the rapeseed supply chain but remains below the vehicle production contribution. Freshwater consumption (Figure 7 (b)) is dominated by vehicle production in all cases, with fuel production as the second contributor. All ammonia-fueled scenarios are about 40–50 % higher than diesel, mainly due to water use in the biodiesel (rapeseed) supply chain. Among ammonia sources, the nuclear pathway has the highest freshwater demand, driven by cooling water use in the nuclear plant.

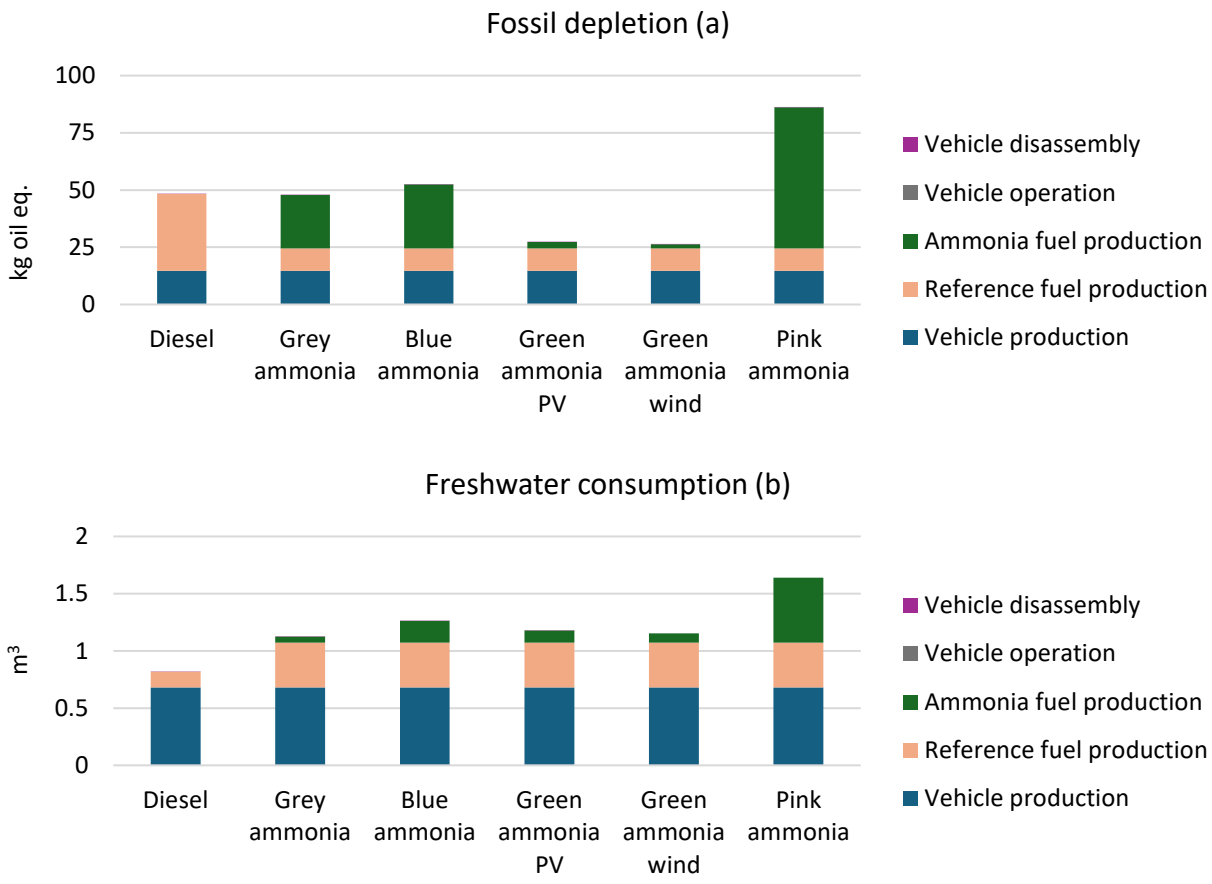

Figure 7. Fossil depletion and freshwater consumption results.

Figure 8 (a) shows results for the human health endpoint. For the diesel case, diesel and vehicle production contribute most, driven by the human toxicity midpoint (a measure of emitted carcinogens in 1.4-dichlorobenzene equivalents). For the ammonia cases, the operation phase dominates, mainly due to elevated NH_3 and NO_2 emissions (treated as secondary PM within ReCiPe), vehicle production follows. Overall, human health impacts are about 47 % higher for ammonia scenarios than for diesel. Figure 8 (b) shows ecosystem quality results. For diesel, vehicle production dominates, followed by diesel production and operation. In the ammonia cases, biodiesel production adds substantially to this category, with impacts around 2.5 times higher than diesel production due to land use from rapeseed cultivation. Ammonia production also contributes, with electrolysis routes highest, especially PV-based electricity, due to terrestrial toxicity from PV manufacturing and EoL. The operation phase is about five times higher for ammonia than for diesel, again driven by elevated NO_x and NH_3 emissions. Overall, the ammonia-fueled mini tractor has roughly twice the ecosystem quality impact of the diesel tractor.

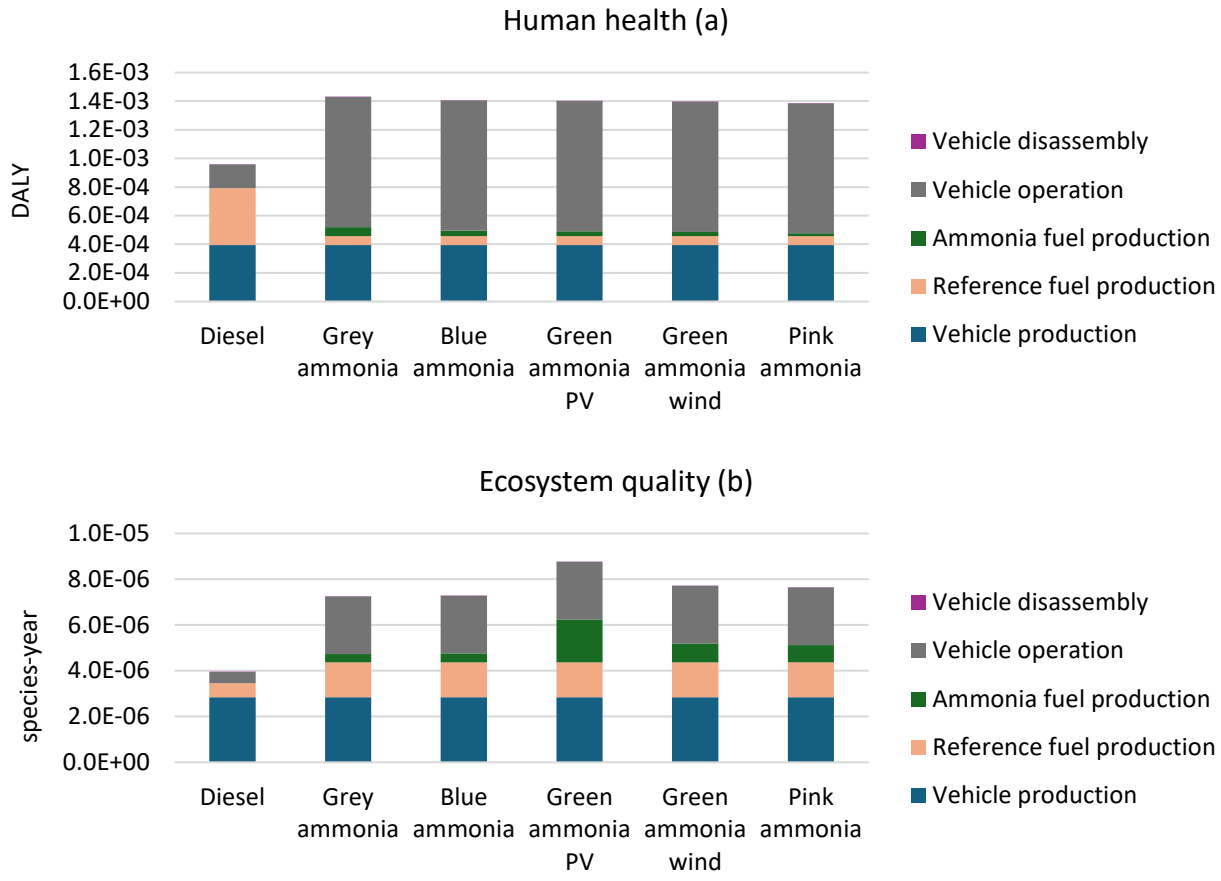

Figure 8. Human health and ecosystem quality results.

Chapter 5 – LCC of an ammonia-fueled mini tractor

The analysis is set from the perspective of a small orchard owner choosing a new mini tractor: (i) a diesel-fueled tractor or (ii) an ammonia-fueled tractor with the same chassis but an engine adapted for port injected NH_3. The difference between the two vehicles lies in the cost of the ammonia setup; dealer distribution and margin are assumed identical. The options are mutually exclusive and are assessed as standalone purchases. The LCC includes capital costs, operating costs (fuel and maintenance), and EoL costs. The analysis primarily uses U.S. market data (treated as international). Fuel costs cover NH_3 (for multiple supply pathways consistent with the LCA) and the biodiesel pilot, while maintenance and EoL are treated in a simplified way as proportional to the purchase cost. All values are expressed in 2024 $.

The adaptation cost is based on inputs from the ACTIVATE project experiments and includes the ammonia tank, fuel line, selective catalytic reduction (SCR) system, and factory service (assembly labor). Operational costs depend on ammonia and biodiesel prices for the ammonia-fueled tractor and diesel price for the diesel-fueled tractor, as well as engine fuel consumption. Annual fuel consumptions are taken from the LCA results (Chapter 4) and are applied directly in the LCC.

Diesel and biodiesel prices come from statistical data [20]. Ammonia costs are determined from cost functions derived from the IEA report [21]. A retail markup is added to convert cost of ammonia to its price, accounting for distribution (fuel transport), storage (facility maintenance), taxes, and retail margin.

The complete LCC assumptions are as follows:

i. Time horizon: 10 years
ii. Diesel/biodiesel: first-year prices are sourced from the U.S. Department of Energy's (2024 average retail) [20]. Change in price over time follows the U.S. Energy Information Administration (EIA) forecasts [22].
iii. Ammonia: for grey and blue ammonia, the initial natural gas price and its trajectory over the years come from the EIA predictions [23]. For electrolysis-based ammonia, the electricity prices are taken from the IEA's Levelised Cost of Electricity (LCOE) Calculator [24], no variation over time is included:
    a. green PV – utility-scale solar PV (median case, 100 MW)
    b. green wind – onshore wind (≥1 MW, median case, 100 MW)
    c. pink – long-term plant operation (10 years, 1000 MW)
iv. A real discount rate of 5 % is applied to all operating cash flows.
v. First year prices are: diesel 1.06 $/l, biodiesel 1.20 $/l, natural gas 4.58 $/MMBtu, electricity from PV 52.7 $/MWh, electricity from wind 46.5 $/MWh, and electricity from nuclear 43.0 $/MWh.

Fuel cost break-even analysis per 1 GJ (LHV basis) is displayed in Figure 9. The following assumptions apply:

i. Green: electrolysis-based ammonia
ii. Grey low: NG-based ammonia at 3.5 $/MMBtu
iii. Grey high: NG-based ammonia at 12 $/MMBtu
iv. Blue low: NG-based ammonia coupled with CCS at 3.5 $/MMBtu
v. Blue high: NG-based ammonia coupled with CCS at 12 $/MMBtu
vi. Diesel low: minimum retail between 2013 and 2023 based on [20], at 0.74 $/l
vii. Diesel high: maximum retail between 2013 and 2023 based on [20], at 1.70 $/l
viii. Biodiesel low: analogously to diesel, at 0.98 $/l
ix. Biodiesel high: analogously to diesel, at 1.71 $/l

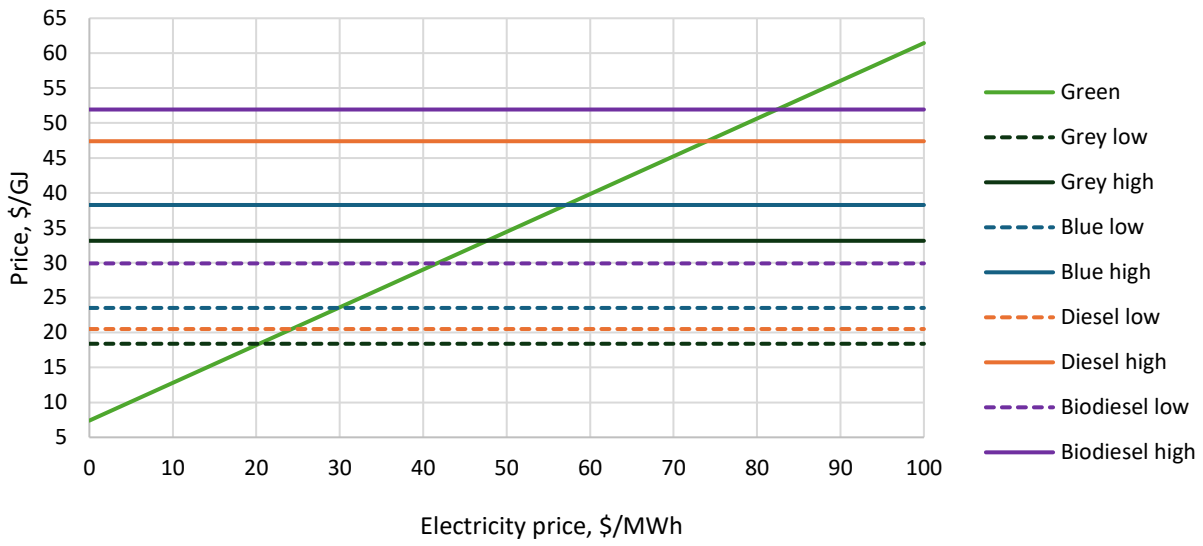

Figure 9. Price comparison of ammonia and other fuels per GJ.

At low gas prices, the break-point electricity price is 20.5 $/MWh versus grey low ammonia and 30 $/MWh versus blue low. IEA's LCOE shows an electricity price of about 40 $/MWh for nuclear (LTO, 1000 MW), onshore wind (≥1 MW), and utility-scale PV under favorable conditions; in such cases, green and pink ammonia cannot compete with NG-based routes. At high gas prices, break-points increase to 47 $/MWh (grey high) and 57 $/MWh (blue high). Under these conditions, green and pink ammonia can undercut NG-based ammonia, but outcomes are case-specific. For diesel, the low price lies between grey low and blue low, giving a green ammonia break-point of 24 $/MWh; at high diesel, the break-point is 74 $/MWh. For biodiesel, the break-points are 42 $/MWh (low) and 82.5 $/MWh (high), making biodiesel generally the costliest option.

The second part of the results concerns the LCC case study. Figure 10 aggregates all cost components for the ammonia-fueled tractor (by ammonia source) and the diesel reference. Baseline refers to the capital cost of the diesel-fueled mini tractor, adaptation to the cost of converting it to ammonia, and pilot fuel to diesel in the diesel case and biodiesel in the ammonia case.

The LCC of the ammonia tractor is around three times that of the diesel tractor, primarily because the capital expenditure of the ammonia-fueled vehicle is about 3.3 times the price of the diesel vehicle. This is driven by equipment and factory services, which account for roughly half of the total capital expenditure of the ammonia-fueled tractor. Pilot fuel cost is higher for the diesel case than for the ammonia case, reflecting greater diesel use compared with the smaller biodiesel pilot requirement. Ammonia itself contributes only 2–3 % of the total LCC. For grey/blue routes, this is due to low NG prices considered (3.15–4.58 $/MMBtu). Electrolysis-based ammonia at 43–53 $/MWh is more expensive than NG-based ammonia at low gas prices, consistent with Figure 9. Since biodiesel is about 1.1 $/l and the ammonia setup still consumes biodiesel as pilot fuel, total

fuel expenditure for the ammonia tractor is about 10–30 % higher than for the diesel tractor, depending on the ammonia production pathway. Maintenance and EoL are modeled as fractions of acquisition cost and are therefore about 3.3 times higher for the ammonia tractor.

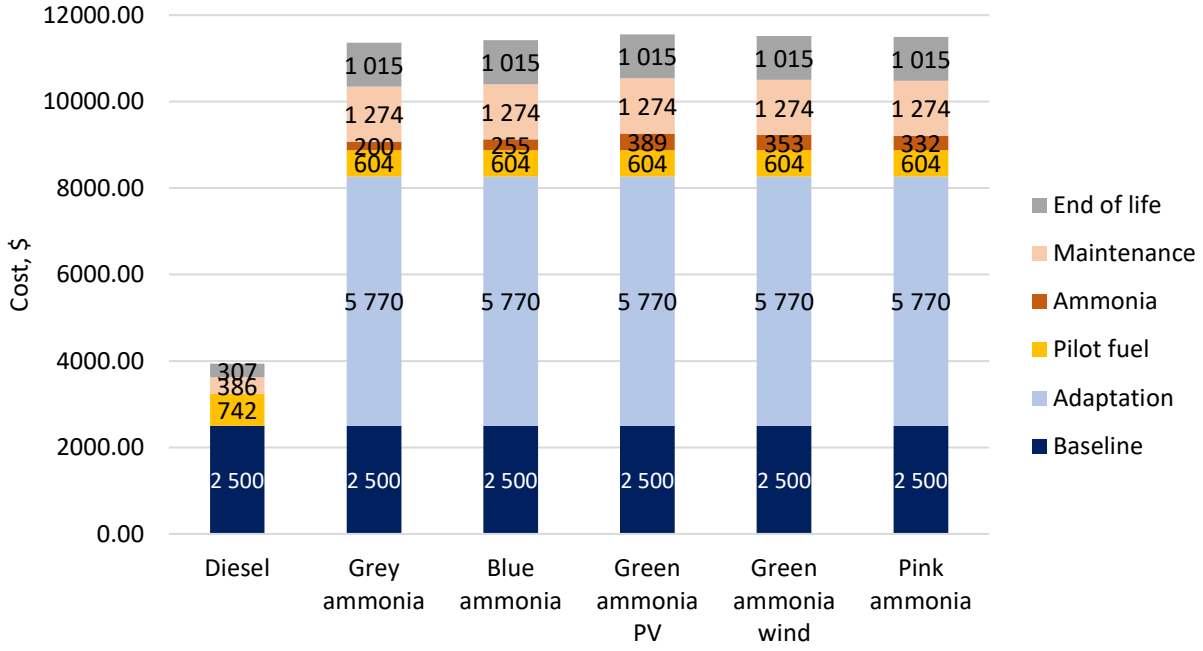

Figure 10. LCC results.

Figure 10 shows that the ammonia-fueled tractor is much more expensive than the diesel reference, mainly because of acquisition costs. However, the bottom-up aggregated capital expenditure may differ from real-world values: high-volume production could lower equipment and factory service costs, while additional safety and control requirements could increase them. Fuel prices are also based on assumptions and forecast trends that may not match future developments. Therefore, LCC results are better expressed as a range than as exact values.

Considering a ± 30 % sensitivity range, as an early-stage estimate range [25], for capital expenditure and fuel price variations according to the LCC assumptions, an LCC interval can be defined and represented by best-case (BS) and worst-case (WS) scenarios.

Best case (BS) – favorable market assumptions:

i. Capital expenditure: –30 % for all items.
ii. Biodiesel: 0.98 $/l.
iii. Natural gas: 3.5 $/MMBtu.
iv. Electricity: 43.0 $/MWh.

Worst case (WS) – adverse market assumptions:

i. Capital expenditure: +30 % for all items.
ii. Biodiesel: 1.71 $/l.
iii. Natural gas: 12 $/MMBtu.
iv. Electricity: 52.7 $/MWh.
v. Ammonia price is increased by carbon-compliance cost at 35 $/t$CO_2$ (grey and blue ammonia) and transport at 70 $/t NH_3 (all ammonia pathways).

Figure 11 compares the BS and WS scenarios. Since ammonia accounts for only about 2–3 % of total LCC in the default case, this trend remains true under BS and WS scenarios. Depending on market conditions, the following can be concluded:

i. Capital expenditure for the ammonia-fueled tractor is 2.3–4.3 times that of the diesel tractor.
ii. Fuel cost (ammonia plus pilot fuel) is 1.1–2.0 times that of the diesel tractor, except for grey ammonia, which can approach diesel fuel cost under low biodiesel and low NG prices.
iii. Maintenance and EoL, modeled as fractions of acquisition cost, are also 2.3–4.3 times higher for the ammonia tractor.

Chapter 6 – Summary

The two primary objectives of this work – (i) evaluating the differences in environmental impacts between an ammonia-fueled and a diesel-fueled mini tractor using life cycle assessment (LCA), and (ii) comparing their economic performance using life cycle costing (LCC) – have been achieved. An environmental impact assessment of ammonia production pathways indicates that, among the pathways analyzed, the preferred option under the climate change criterion is electrolysis-based ammonia produced using nuclear electricity. However, its high freshwater consumption and fossil depletion (driven by uranium use included in this category within the ReCiPe method) can be limiting, particularly in water-scarce or resource-constrained regions. In such contexts, wind-powered electrolysis may be more suitable: it substantially lowers impacts in these two categories while maintaining a low climate change burden, which is the main motivation for alternative fuels. Relative to diesel, all ammonia pathways except grey (SMR without CCS) meet the decarbonization objective, with blue ammonia offering only modest improvement. At the endpoint level, vehicle fueled with ammonia produced using nuclear or wind electricity shows the lowest human health impact. However, regardless of the ammonia production pathway, it worsens ecosystem quality relative to diesel, with PV-based ammonia performing particularly poorly in this category. Engine performance analysis shows that although the ammonia-fueled engine emits less CO_2 than the diesel case, significant NO_x and N_2O formation occurs, especially at partial load.

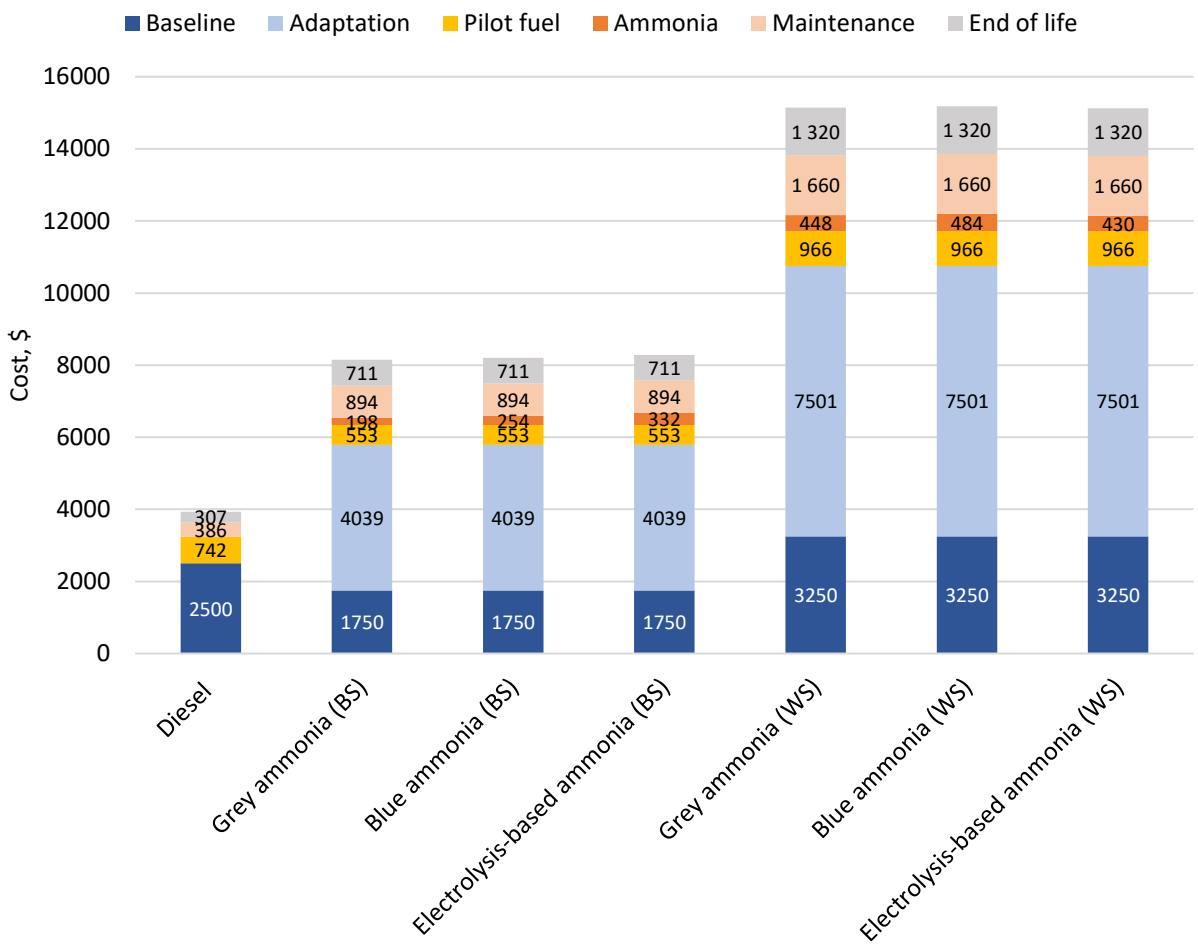

Figure 11. Range of estimated LCC results.

The premise that ammonia can support decarbonization of ICEs – by being produced renewably and combusting without carbon emissions – has been confirmed for the orchard mini tractor case, but the magnitude of the benefit depends on engine operation. Compared to diesel, the ammonia-fueled vehicle examined here shows lower operational GHG emissions (about 72 kg CO_2 eq. versus about 88 kg CO_2 eq., an 18 % reduction limited by N_2O formation and the CO_2 from the pilot fuel). Over the full life cycle, switching to ammonia with a biodiesel pilot fuel reduces climate change impacts more strongly – by 42–44 % – when ammonia is produced from wind or nuclear power and the biodiesel footprint is included. For fossil depletion, solar- and wind-derived ammonia used in the ammonia-fueled vehicle achieves 43–45 % reductions, whereas nuclear-based ammonia increases depletion by around 78 %. Freshwater consumption is 40–50 % higher across all ammonia routes than for diesel, with the nuclear pathway approaching a twofold increase. Ammonia vehicle scenarios increase human health impacts by around 47 % relative to diesel, mainly due to secondary particulates from NH_3/NO_x, and roughly double the ecosystem quality impact, resulting from both operational emissions and fuel production burdens.

Overall, for climate change, nuclear-based ammonia performs best, but its high fossil depletion and water use must be considered in long-term resource planning and in water-stressed areas. Green wind ammonia has only slightly higher climate change impacts but much lower fossil depletion and freshwater consumption. It may therefore be cautiously identified as the most balanced option. Nevertheless, endpoint results show that elevated NO_x and NH_3 emissions from combustion must be addressed, since in all scenarios the ammonia-fueled mini tractor performs worse than diesel in terms of human health and ecosystem quality.

The LCC assessment has identified the conditions under which an ammonia-fueled mini tractor could become competitive with a diesel-fueled vehicle. First, the cost ranking between natural gas-based and electrolysis-based ammonia shows that at low gas prices (3.5 $/MMBtu), electrolysis would require electricity below roughly 20–30 $/MWh, which is unlikely in most contexts. At higher gas prices (12 $/MMBtu), electrolysis-based ammonia can become cheaper if electricity is about 47–57 $/MWh, which is achievable in favorable renewable or nuclear cases (around 40–46 $/MWh). Second, compared with diesel: at a low diesel price (0.74 $/l), only natural-gas-based ammonia at low gas prices is competitive; electrolysis would need electricity under 24 $/MWh, which is improbable. At a high diesel price (1.70 $/l), cost parity is possible if electricity remains below 74 $/MWh, which is feasible in many cases.

In the LCC case study, the capital expenditure of the ammonia-fueled mini tractor is about 3.3 times higher than that of the standard diesel vehicle under the stated assumptions. Combined fuel costs for the ammonia tractor are 10–30 % higher than for diesel; this gap can be reduced by lowering ammonia or biodiesel prices, with a reduction in biodiesel price being particularly effective since it dominates the combined fuel expenditure. Accounting for capital expenditure uncertainty and fuel price volatility, the LCC of the ammonia-fueled tractor is estimated at roughly 2–4 times that of the diesel mini tractor. To lower this difference, policymakers could offer incentives for carbon-free vehicles to compensate orchard owners for the high acquisition costs of a new vehicle.

References

[1] Global Change Data Lab, “Global direct primary energy consumption,” Our World in Data. Accessed: Oct. 10, 2025. [Online]. Available: https://ourworldindata.org/grapher/global-primary-energy

[2] “Higher Calorific Values of Common Fuels: Reference & Data,” The Engineering ToolBox. Accessed: July 16, 2025. [Online]. Available: https://www.engineeringtoolbox.com/fuels-higher-calorific-values-d_169.html

[3] T. Abbasi and S. A. Abbasi, "'Renewable' hydrogen: Prospects and challenges," *Renewable and Sustainable Energy Reviews*, vol. 15, no. 6, pp. 3034–3040, Aug. 2011, doi: 10.1016/j.rser.2011.02.026.
[4] "Hydrogen - Density and Specific Weight vs. Temperature and Pressure," The Engineering ToolBox. Accessed: July 16, 2025. [Online]. Available: https://www.engineeringtoolbox.com/hydrogen-H2-density-specific-weight-temperature-pressure-d_2044.html
[5] H. T. Hwang and A. Varma, "Hydrogen storage for fuel cell vehicles," *Current Opinion in Chemical Engineering*, vol. 5, pp. 42–48, Aug. 2014, doi: 10.1016/j.coche.2014.04.004.
[6] "Ammonia - NH3 - Thermodynamic Properties," The Engineering ToolBox. Accessed: July 16, 2025. [Online]. Available: https://www.engineeringtoolbox.com/ammonia-d_971.html
[7] "Ammonia - Properties at Gas-Liquid Equilibrium Conditions," The Engineering ToolBox. Accessed: July 16, 2025. [Online]. Available: https://www.engineeringtoolbox.com/ammonia-gas-liquid-equilibrium-condition-properties-temperature-pressure-boiling-curve-d_2013.html
[8] A. J. Reiter and S.-C. Kong, "Demonstration of Compression-Ignition Engine Combustion Using Ammonia in Reducing Greenhouse Gas Emissions," *Energy Fuels*, vol. 22, no. 5, pp. 2963–2971, Sept. 2008, doi: 10.1021/ef800140f.
[9] C. Tornatore, L. Marchitto, P. Sabia, and M. De Joannon, "Ammonia as Green Fuel in Internal Combustion Engines: State-of-the-Art and Future Perspectives," *Front. Mech. Eng.*, vol. 8, p. 944201, July 2022, doi: 10.3389/fmech.2022.944201.
[10] P. Dimitriou and R. Javaid, "A review of ammonia as a compression ignition engine fuel," *International Journal of Hydrogen Energy*, vol. 45, no. 11, pp. 7098–7118, Feb. 2020, doi: 10.1016/j.ijhydene.2019.12.209.
[11] M.-C. Chiong *et al.*, "Advancements of combustion technologies in the ammonia-fuelled engines," *Energy Conversion and Management*, vol. 244, p. 114460, Sept. 2021, doi: 10.1016/j.enconman.2021.114460.
[12] United States Environmental Protection Agency (EPA), "Understanding Global Warming Potentials," United States Environmental Protection Agency. Accessed: Oct. 13, 2025. [Online]. Available: https://www.epa.gov/ghgemissions/understanding-global-warming-potentials
[13] European Commission, Joint Research Centre (JRC), Institute for Environment and Sustainability, "International Reference Life Cycle Data System (ILCD) Handbook – General guide for Life Cycle Assessment – Detailed guidance," European Commission, Joint Research Centre (JRC), Luxembourg, ILCD Handbook, 2010.
[14] P. Iradukunda, E. M. Mwanaumo, and J. Kabika, "A review of integrated multicriteria decision support analysis in the climate resilient infrastructure development," *Environmental and Sustainability Indicators*, vol. 20, p. 100312, Dec. 2023, doi: 10.1016/j.indic.2023.100312.
[15] Sphera Solutions, Inc., "Search Life Cycle Assessment Datasets," Sphera. Accessed: Oct. 13, 2025. [Online]. Available: https://lcadatabase.sphera.com/

[16] Y. Bicer, I. Dincer, C. Zamfirescu, G. Vezina, and F. Raso, "Comparative life cycle assessment of various ammonia production methods," *Journal of Cleaner Production*, vol. 135, pp. 1379–1395, Nov. 2016, doi: 10.1016/j.jclepro.2016.07.023.
[17] S. Ghavam, M. Vahdati, I. A. G. Wilson, and P. Styring, "Sustainable Ammonia Production Processes," *Front. Energy Res.*, vol. 9, p. 580808, Mar. 2021, doi: 10.3389/fenrg.2021.580808.
[18] S. Morais, T. M. Mata, A. A. Martins, G. A. Pinto, and C. A. V. Costa, "Simulation and life cycle assessment of process design alternatives for biodiesel production from waste vegetable oils," *Journal of Cleaner Production*, vol. 18, no. 13, pp. 1251–1259, Sept. 2010, doi: 10.1016/j.jclepro.2010.04.014.
[19] University of Maine, "Calendar of Apple Orchard Management Activities," Cooperative Extension: Garden and Yard. Accessed: Oct. 18, 2024. [Online]. Available: https://extension.umaine.edu/gardening/manual/calendar-apple-orchard-management-activities/
[20] "Alternative Fuels Data Center," U.S. Department of Energy, Energy Efficiency & Renewable Energy. Accessed: Jan. 23, 2025. [Online]. Available: https://afdc.energy.gov/fuels/prices.html
[21] IEA, "The Future of Hydrogen," June 2019. [Online]. Available: https://www.iea.org/reports/the-future-of-hydrogen
[22] "Annual Energy Outlook 2023 Table: Table 12. Petroleum and Other Liquids Prices," U.S. Energy Information Administration. Accessed: Jan. 24, 2025. [Online]. Available: https://www.eia.gov/outlooks/aeo/data/browser/#/?id=12-AEO2023&region=0-0&cases=ref2023&start=2021&end=2050&f=A&linechart=ref2023-d020623a.3-12-AEO2023~&map=&ctype=linechart&sourcekey=0
[23] "Annual Energy Outlook 2023 Table: Table 13. Natural Gas Supply, Disposition, and Prices," U.S. Energy Information Administration. Accessed: Jan. 24, 2025. [Online]. Available: https://www.eia.gov/outlooks/aeo/data/browser/#/?id=13-AEO2023&cases=ref2023&sourcekey=0
[24] IEA, "Levelised Cost of Electricity Calculator." Accessed: Jan. 24, 2025. [Online]. Available: https://www.iea.org/data-and-statistics/data-tools/levelised-cost-of-electricity-calculator
[25] AACE International, "Cost Estimate Classification System – As Applied in Engineering, Procurement, and Construction for the Process Industries," AACE International, Recommended Practice 18R-97, rev 2016.